

evidence has been published. Geometrical factors, as well as the absence of clean surfaces, seriously hamper such observations.

## REFERENCES AND NOTES

1. S. Iijima, *Nature* **354**, 56 (1991).
2. R. F. Curl and R. E. Smalley, *Sci. Am.* **265**, 32 (October 1991).
3. M. S. Dresselhaus, G. Dresselhaus, R. Saito, *Phys. Rev. B* **45**, 6234 (1992).
4. X. F. Zhang et al., *J. Cryst. Growth* **130**, 368 (1993).
5. X. B. Zhang, X. F. Zhang, S. Amelinckx, G. Van Tendeloo, J. Van Landuyt, *Ultramicroscopy* **54**, 237 (1994).
6. Z. G. Li, P. J. Fagan, L. Liang, *Chem. Phys. Lett.* **207**, 148 (1993).
7. M. Liu and J. M. Cowley, *Ultramicroscopy* **53**, 333 (1994).
8. ———, *Carbon* **32**, 393 (1994).
9. R. Bacon, *J. Appl. Phys.* **31**, 283 (1960).
10. O. Zhou et al., *Science* **263**, 1744 (1994).
11. T. W. Ebbesen, *Annu. Rev. Mater. Sci.* **24**, 235 (1994).
12. J. C. Charlier and J. P. Michenaud, *Phys. Rev. Lett.* **70**, 1858 (1993).
13. A. M. Kosevich, in *Dislocations in Solids*, F. R. N. Nabarro, Ed. (North-Holland, Amsterdam, 1979), vol. 1, pp. 66–67.
14. L. Margulis, J. L. Hutchison, R. Tenne, in *Electron Microscopy 1994*, proceedings of the 13th International Conference on Electron Microscopy, Paris, 17 to 22 July 1994, B. Joffrey and C. Colliex, Eds. (Les éditions de physique, Paris, 1994), vol. 2A, p. 317.
15. V. P. Dravid et al., *Science* **259**, 1601 (1993).
16. P. M. Ajayan, T. Ichihashi, S. Iijima, *Chem. Phys. Lett.* **202**, 384 (1993).
17. S. Amelinckx, W. Luyten, T. Krekels, G. Van Tendeloo, J. Van Landuyt, *J. Cryst. Growth* **121**, 543 (1992).
18. S. Iijima, *Mater. Sci. Eng. B* **19**, 172 (1993).
19. ——— and T. Ichihashi, *Nature* **363**, 603 (1993).
20. The order of magnitude of the relative change in the  $c$  parameter due to stresses will be at most  $(\alpha_{\perp} - \alpha_{\parallel})\Delta T$ . With  $\alpha_{\perp} - \alpha_{\parallel} \approx 10^{-5}/\text{K}$  [B. T. Kelly, in *Materials Science and Technology*, R. W. Cahn, P. Haasen, E. J. Kramer, Eds. (VCH, Weinheim, 1994), vol. 10A, part 1, p. 383] and  $\Delta T \approx 3 \times 10^3$  to  $4 \times 10^3$  K, one finds  $\Delta c/c \approx 0.03$  to  $0.04$ .
21. Y. Saito, T. Yoshikawa, S. Bandow, M. Tomita, T. Hayashi, *Phys. Rev. B* **48**, 1907 (1993).
22. This work was funded in part by the Belgian National Program of Inter-University Research Projects initiated by the State Prime Minister Office (Science Policy Programming). We also acknowledge funding from the National Fund for Scientific Research.

2 September 1994; accepted 6 December 1994

# Synthesis and Characterization of Anisometric Cobalt Nanoclusters

Charles P. Gibson\* and Kathy J. Putzer

Sonication of aqueous  $\text{Co}^{2+}$  and hydrazine resulted in the formation of anisometric (disk-shaped) cobalt nanoclusters that averaged about 100 nanometers in width and 15 nanometers in thickness. Electron diffraction from single particles revealed that they were oriented (001) crystals that conformed to a trigonal or hexagonal unit cell four times the size of the cell adopted by bulk  $\alpha$ -cobalt. Lorentz microscopy indicated that these were single-magnetic domain particles, with the axis of magnetization located in the (101) plane, offset at some appreciable angle from the (001) axis.

Small magnetic particles (magnetic nanoclusters) are of immense technological importance because of their use in magnetic recording media and in the construction of permanent magnets (1, 2). Desirable characteristics for these materials include sufficient shape and magnetocrystalline anisotropy so that a preferred magnetic field orientation is adopted in the final product. Ideally, the nanoclusters would be monodisperse and magnetically hard, and each particle would contain a single magnetic domain.

Of the three transition metals that are normally ferromagnetic (Fe, Co, and Ni), oriented nanoclusters of cobalt probably have the greatest potential for use because  $\alpha$ -cobalt (unlike iron and nickel) is uniaxial (2, 3). Unfortunately, however, facile syntheses leading to anisometric cobalt nanoclusters have not yet been reported (4). Herein we describe such a synthesis: a facile

and inexpensive procedure that leads to oriented, anisometric, single-domain ferromagnetic cobalt nanoclusters.

Initial attempts to synthesize colloidal cobalt at moderate temperature ( $\leq 100^\circ\text{C}$ ) by reduction of  $\text{Co}^{2+}(\text{aq})$  with hydrazine were unsuccessful, presumably because of the kinetic stability of the system (5–7). Because the attempted reaction was, in theory, thermodynamically allowed and quite exothermic (7, 8), we reasoned that a self-sustaining reaction might be initiated by the application of high-intensity ultrasound.

When basic solutions containing  $\text{Co}^{2+}$  and hydrazine were sonicated, there was, following a short induction period, a sudden color change (blue-violet to silver-gray) as a result of the formation of colloidal cobalt. The colloidal cobalt nanoclusters were allowed to flocculate and, under the influence of gravity, fall to the bottom of the reactor. Most of the liquid in the reactor was removed by means of a cannula and was then replaced with water. The particles were resuspended and allowed to flocculate and set-

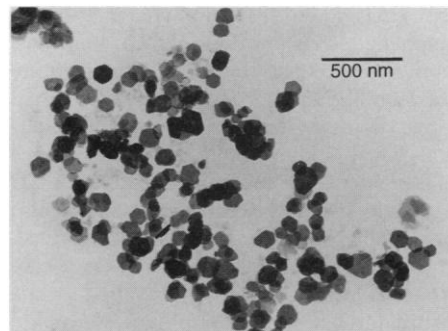


**Fig. 1.** A group of cobalt nanoclusters. The particles, which adopt a hexagonal or centered trigonal unit cell, are preferentially deposited as oriented (001) plates.

tle once again, whereupon most of the liquid was removed. This washing process was repeated until the pH of the removed water was between 7 and 8. At this point, the hydrated floc was either stored for later use or the water was removed under a stream of dry nitrogen (or under vacuum) to give a free-flowing gray powder (9, 10). Both the hydrated floc and the free-flowing gray powder were ferromagnetic. Assays of the gray powder by atomic absorption and energy dispersive x-ray spectroscopy (EDS) showed that it consisted primarily of cobalt (98.3%). A small amount of oxygen was also present, presumably in the form of a very thin oxide coating (10, 11). No other impurities were present in quantities measurable by EDS. Samples that were to be characterized by transmission electron microscopy (TEM), Lorentz electron microscopy, and selected area electron diffraction (SAD) were prepared from the hydrated floc. The floc was dispersed by sonication and then deposited on a Formvar or collodion-coated TEM grid.

It is significant to note that, when handled properly, samples of the hydrated floc could be stored (under nitrogen) and effectively resuspended for at least several days after the initial synthesis. This property was a bit surprising because ferromagnetic particles tend to form tight aggregates as a result of magnetic attractions between the particles (1, 12). However, the cobalt nanoclusters are small enough to be strongly influenced by Brownian forces. Because of the shape anisotropy of the particles, these forces result in the rotation of the particles (Brownian rotation). This effect probably inhibits the intimate contact between particles that is necessary for agglomeration (13, 14).

Examination of the product by TEM revealed that it consisted of anisometric (disk-like) nanoclusters that were more or less hexagonal in shape. A photomicrograph of a typical product (Fig. 1) illustrates the morphology of the particles and shows their orientation with respect to the polymer-coated TEM grid. We see from this image that the

Department of Chemistry, University of Wisconsin, Oshkosh, WI 54901, USA.

\*To whom correspondence should be addressed.

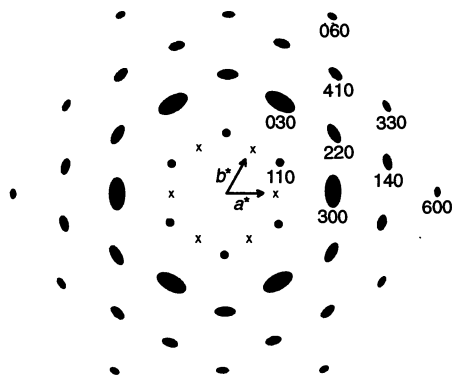


**Fig. 2.** A digitized, computer-enhanced SAD pattern from a single cobalt nanocluster. This pattern indicates a hexagonal or centered trigonal unit cell with  $a = 5.06 \text{ \AA}$ , rather than the hexagonal cell  $a = 2.507 \text{ \AA}$  normally adopted by bulk cobalt.

particles adopt a preferred orientation: The majority of the particles in this image were deposited so as to be coplanar with the polymeric support (204 of 206; 99%). The average width for all particles in this image (measured at the widest point of each) was 99 nm ( $\sigma = 25 \text{ nm}$ ). Only two of the particles in this sample (2 of 206; 1%) were oriented "on edge." Based on measurements of these two particles, the typical thickness was estimated to be  $\sim 15 \text{ nm}$ .

The SAD patterns from isolated single cobalt nanoclusters (Figs. 2 and 3) exhibited hexagonal symmetry with numerous absences. These patterns were consistent with  $hk0$  data from a trigonal or hexagonal cell with  $a = 5.08 \text{ \AA}$ . The fact that data satisfying  $h - k + l \neq 3n$  were systematically absent ( $l = 0$  in this case) limits the possible space groups to a relatively small number of hexagonal or centered trigonal groups (15). A very weak reflection located halfway between the 000 and 003 reciprocal lattice points indicated an as yet unidentified lattice modulation (16). On very large aggregates of particles, SAD gave rings (or spotty rings), most of which corresponded to  $hk0$  reflections. However, several rings that corresponded to more general  $hkl$  reflections were observed and were used to determine the  $c$  lattice constant. These ring patterns confirmed that  $a = 5.06 \text{ \AA}$  and indicated that  $c = 4.07 \text{ \AA}$ . The presence of only  $hk0$  data in the single-crystal SAD patterns, and primarily  $hk0$  data in the powder patterns, is significant because it shows that the particles adopted a preferred (001) orientation when deposited onto a polymer film. This property, in turn, is important because oriented ferromagnetic particles are generally required for high-density magnetic storage media (1, 2).

The structure of the cobalt nanoclusters differs from that adopted by bulk  $\alpha$ -cobalt (17). Whereas bulk  $\alpha$ -cobalt is hexagonal close packed ( $P6_3/mmc$  symmetry) with  $a =$

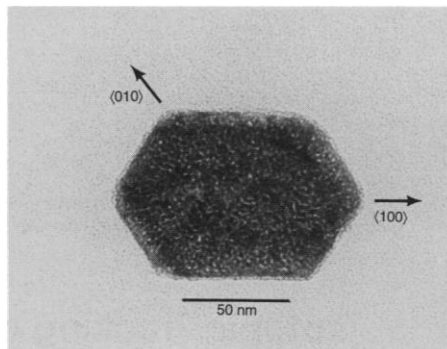


**Fig. 3.** A single cobalt nanocluster. The orientations of the  $\langle 100 \rangle$  and  $\langle 010 \rangle$  zone axes were determined by SAD and TEM.

$2.507 \text{ \AA}$  and  $c = 4.069 \text{ \AA}$ , the anisometric nanocluster conformed to a hexagonal or centered trigonal unit cell with  $a = 5.06 \text{ \AA}$  and  $c = 4.07 \text{ \AA}$ . This suggests that the lattice of the nanocluster is derived from the hexagonal cell of  $\alpha$ -cobalt by a distortion that doubles the  $a$  axis. Although the exact nature of this distortion is (as yet) unknown, we speculate that it may be a result of a distortion caused by the oxide coating. Although this coating is certainly present on both the nanocluster form and bulk  $\alpha$ -cobalt (11, 17), its influence on the bulk is probably negligible because most bulk cobalt atoms are quite far from the surface. In contrast, all cobalt atoms in the anisometric nanoclusters are within  $\sim 15$  unit cells of the coating. For these materials, the effect of the surface distortion may very well extend through the entire crystal.

The magnetic structure of these particles is of considerable interest to us because magnetic structure may ultimately determine any practical use for these particles (1). The most important issue to settle is whether the cobalt nanoclusters contain a single or multiple magnetic domains. Simple calculations based on the structure and properties of bulk  $\alpha$ -cobalt suggested that cobalt disks measuring 100 nm by 15 nm could not be single-domain particles (2, 18). However, these calculations ignored the fact that magnetic hardness usually is much larger for colloidal materials than for bulk (19), and they overlooked the fact that the axis of magnetization in the nanoclusters need not coincide with the crystallographic  $c$  axis as it does in  $\alpha$ -cobalt at room temperature (2, 20). For example, if the magnetization axis were oriented along the  $a$  axis, our calculations suggest that cobalt platelets as large as 200 nm by 30 nm might still exist as single-magnetic domain particles. Because of the uncertainty inherent in these calculations, we chose to investigate this issue experimentally by Lorentz electron microscopy.

Electrons that are traveling through a magnetic field experience Lorentz forces.

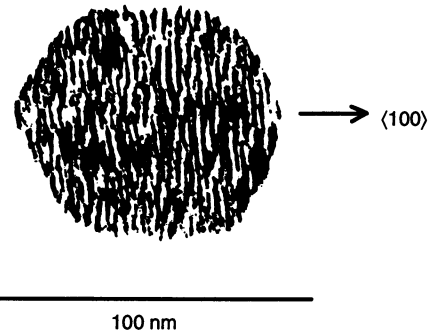


**Fig. 4.** Lorentz electron microscopy was used to investigate the magnetic structure of this particle. This image, which was digitized and computer enhanced, shows that the particle is a single domain and that the projection of the magnetization axis onto the image plane is along the  $\langle 100 \rangle$  direction.

Because electrons traveling through different magnetic regions experience differing Lorentz forces, they follow slightly different trajectories. As a consequence, the electrons are slightly out of phase when combined to form an image. Under conditions of normal focus, these differences are much too small to contribute to contrast in the image. However, if further phase shifts are introduced, for example by appropriate defocusing (Fresnel imaging), the combined phase shifts are sufficient to give added image contrast. In this manner, information concerning the magnetic structure can be produced in the image (16, 21). Figure 4 shows a typical cobalt particle that was imaged under Fresnel conditions (22). In this case, magnetic fine structure was revealed by ripples that run through this sample. The fact that the ripples all run in the same general direction is compelling evidence that the particle consists of a single magnetic domain.

Because only the component of the magnetic field perpendicular to the electron trajectory gives rise to the Lorentz effect, the ripple-like patterns in Lorentz electron microscopy reveal the projection of the magnetization axis onto the imaging plane (15, 21). In this case, the projection of the magnetization axis (which is perpendicular to the ripples) was in the  $\langle 100 \rangle$  direction. Unlike bulk  $\alpha$ -cobalt, in which the magnetization axis is along the  $\langle 001 \rangle$  direction, the magnetization axis in the cobalt nanocluster is in the (101) plane, but offset from the  $\langle 001 \rangle$  axis at some significant angle.

The cobalt nanoclusters described here have a number of characteristics that might make them useful in the construction of high-density recording media or permanent magnets. (i) They can be easily synthesized from relatively inexpensive reagents. (ii) They can be stored as a hydrated floc, which can be redispersed. (iii) They are single-magnetic domain entities. (iv) They show considerable shape and magne-

tocrystalline anisotropy. Finally, (v) they adopt a preferred orientation when deposited onto a polymeric film.

## REFERENCES AND NOTES

- M. Ozaki, *Mater. Res. Soc. Bull.* **14**, 35 (1989).
- D. Jiles, *Introduction to Magnetism and Magnetic Materials* (Chapman and Hall, New York, 1991); R. S. Tebble and D. J. Craik, *Magnetic Materials* (Wiley-Interscience, New York, 1969).
- Y. Maeda and M. Takahashi, in *Recent Advances in Magnetism and Magnetic Materials* (World Scientific, Singapore, 1990), pp. 202–213.
- Oriented cobalt films have been synthesized by metal vapor deposition, dc magnetron sputtering, and other techniques. In some cases, oriented cobalt nanoclusters may precipitate from an alloy film. In this situation, however, the cobalt nanoclusters were generated in situ and were not generally suitable for subsequent use in the construction of a device. See, for example, J. R. Childress and C. L. Chien, *J. Appl. Phys.* **70**, 5885 (1991).
- Other researchers have noted that these reactants do not react, or at best react very slowly, under these conditions [I. R. Collins and S. E. Taylor, *J. Dispersion Sci. Technol.* **12**, 403 (1991); D. M. Littrell, D. H. Bowers, B. J. Tatarchuk, *Faraday. Trans. 1* **83**, 3271 (1987); R. S. Sapieszko and E. Matijevic, *Corrosion* **36**, 522 (1980)].
- The reaction can be catalyzed by Pd<sup>2+</sup>(aq), but Co-coated Pd particles would be formed [E. Matijevic, A. M. Poskanzer, P. Zuman, *Plating Surf. Finish.* **1975**, 958 (1975); A. Warshawsky and D. A. Upson, *Polymer* **30**, 972 (1989); S. Harada, T. Kobayashi, Y. Nishizawa, *Funtai Oyobi Funmatsuyakin* **25**, 80 (1978)].
- L. F. Audrieth and B. A. Ogg, *The Chemistry of Hydrazine* (Wiley, New York, 1951).
- Based on standard reduction potentials,  $\Delta G \approx -54$  kJ/mol. Although reactions were not run under standard conditions, it seems reasonably safe to assume that  $\Delta G \ll 0$ . Estimates based on relative bond energies, energy of hydration of Co<sup>2+</sup>, and lattice energy by bulk Co lead to the conclusion that  $\Delta H \ll 0$  as well.
- In a typical synthesis, a blue-violet solution containing both Co(OH)<sub>2</sub><sup>2-</sup> and hydrazine was prepared from CoCl<sub>2</sub>·6H<sub>2</sub>O (25 mg), water (3 ml), a 50% aqueous solution of NaOH (1 ml), and an 85% solution of N<sub>2</sub>H<sub>4</sub>·H<sub>2</sub>O (1 ml). The product was purified and stored under nitrogen.
- Black powders were obtained when the product was not protected from oxygen. These powders had high oxygen content (about 5 to 10%), which suggested the formation of a thick coating of cobalt oxide.
- L. Yiping, G. C. Hadjipanayis, C. M. Sorenson, K. J. Klabunde, *J. Appl. Phys.* **67**, 4502 (1990).
- P. C. Scholten, *J. Magn. Magn. Mater.* **39**, 99 (1988).
- D. H. Everett, *Basic Principles of Colloid Science* (Royal Society of Chemistry, London, 1988).
- When the floc was exposed to an external magnetic field, or upon ultracentrifugation of the floc, irreversible agglomeration occurred. Apparently, these conditions forced intimate contact between particles. The resulting aggregates were (more or less) spherical in shape and about 1 to 10 μm in diameter.
- N. F. M. Henrey and K. Lonsdale, Eds., *International Tables for X-Ray Crystallography*, vol. 1 (Kynoch, Birmingham, AL, 1965).
- J. W. Edington, *Practical Electron Microscopy in Materials Science* (TechBooks, Herndon, VA, 1976).
- A. R. West, *Solid State Chemistry* (Wiley, New York, 1984); J. W. Mellor, *Inorganic and Theoretical Chemistry* (Longmans Green, London, 1965).
- These calculations indicate that plates with a width/thickness ratio of 6.7 would be single domain only when width is below 40 nm. See references cited in (3) for guidelines concerning these calculations.
- W. Gong, H. Li, Z. Zhao, J. Chen, *J. Appl. Phys.* **69**, 5119 (1991).
- D. Gibord, Q. Lu, M. F. Rossignol, in *Science and Technology of Nanostructured Magnetic Materials*, G. C. Hadjipanayis and G. A. Prinz, Eds. (Plenum, New York, 1991), pp. 635–656; S. Ohnuma, A. Kuni-moto, T. Masumoto, *J. Appl. Phys.* **63**, 4243 (1988).
- P. J. Grundy and R. S. Tebble, *Adv. Phys.* **17**, 153 (1968); R. H. Wade, in *Advances in Optical and Electron Microscopy*, R. Barer and V. E. Cosslett, Eds. (Academic Press, New York, 1973), vol. 5, pp. 239–296.
- Lorentz microscopy was conducted on a Zeiss EM10CA TEM instrument, which was operating in the low magnification mode.
- Support of this project was provided by Research Corporation and the University of Wisconsin–Oshkosh Faculty Development Program. The purchase of electron microscopes and an EDS attachment used in this study was made possible by contributions by the National Science Foundation (ILL-8950625) and by a very generous anonymous donor. A. D. Rae is thanked for helpful comments concerning the structure of the cobalt nanocluster. This report is dedicated to L. F. Dahl to mark the occasion of his 65th birthday.

13 October 1994; accepted 5 January 1995

## Isotopic Tracking of Change in Diet and Habitat Use in African Elephants

Paul L. Koch,\* Jennifer Heisinger, Cynthia Moss, Richard W. Carlson, Marilyn L. Fogel, Anna K. Behrensmeyer

The carbon, nitrogen, and strontium isotope compositions of elephants in Amboseli Park, Kenya, were measured to examine changes in diet and habitat use since the 1960s. Carbon isotope ratios, which reflect the photosynthetic pathway of food plants, record a shift in diet from trees and shrubs to grass. Strontium isotope ratios, which reflect the geologic age of bedrock, document the concentration of elephants within the park. The high isotopic variability produced by behavioral and ecological shifts, if it is representative of other East African elephant populations, may complicate the use of isotopes as indicators of the source region of ivory.

In many African parks and reserves, woodlands have been replaced by grasslands in recent decades (1). Potential causes of this transformation include changes in climate, fire frequency, and feeding by large ungulates such as elephants (*Loxodonta africana*) (1, 2). At the same time, poaching and human land use near parks have altered ungulate migration and habitat use patterns, often accelerating vegetation change within protected areas (1, 2). Knowledge of foraging and habitat use patterns in ungulates, and of recent changes in these patterns, are essential to understand controls on ecological transformation and to develop robust conservation strategies. Typically, such data have been gathered through long-term observation (3). Isotopic analysis offers an alternate source of information on diet, habitat, and migration that can be collected rapidly from living or dead animals (4). Isotope composition has also been proposed as a marker to indicate the source region of

ivory, for use in wildlife forensics (5).

Most carbon, nitrogen, and strontium in herbivores are derived from food plants. Because a herbivore's isotopic composition is similar to that of its food, isotopic differences in diet are reflected in herbivore tissues (6, 7). For example, African trees and most shrubs, herbs, and cool-climate grasses are C<sub>3</sub> plants, with low δ<sup>13</sup>C values (≈−27 per mil), whereas warm-climate grasses are C<sub>4</sub> plants, with less negative values (≈−13 per mil) (8). Consequently, the δ<sup>13</sup>C value of collagen (the major protein in bones and ivory) reflects the proportion of browse (leaves, twigs, and shrubs) to grass in the diet (4, 5). The N isotope compositions of plants and herbivores covary with rainfall abundance, and isotope ratios are high in arid regions and low in wet regions (7, 9). Finally, <sup>87</sup>Sr is produced by radioactive decay of <sup>87</sup>Rb, whereas <sup>86</sup>Sr is a stable isotope. Soils have variable <sup>87</sup>Sr/<sup>86</sup>Sr ratios, depending on the initial Rb/Sr ratio and the age of the underlying bedrock. Soils are the source of Sr in plants, which in turn supply the Sr that is deposited in bone and tooth mineral. Overall, animals in areas with old granitic crust have high Sr isotope ratios; in areas with young volcanic rocks or marine sediments, animals have low values (5).

Here we examine the isotopic ecology of elephants from Amboseli National Park, Kenya, to address the degree to which the bones and teeth of Amboseli elephants preserve an isotopic record of changes in diet

P. L. Koch and J. Heisinger, Department of Geological and Geophysical Sciences, Princeton University, Princeton, NJ 08544, USA.

C. Moss, African Wildlife Foundation, Post Office Box 48177, Nairobi, Kenya.

R. W. Carlson, Department of Terrestrial Magnetism, Carnegie Institution of Washington, Washington, DC 20015, USA.

M. L. Fogel, Geophysical Laboratory, Carnegie Institution of Washington, Washington, DC 20015, USA.

A. K. Behrensmeyer, Department of Paleobiology, National Museum of Natural History, Smithsonian Institution, Washington, DC 20560, USA.

\*To whom correspondence should be addressed.